

Unidirectional self-patterning of CaF₂ nanorod arrays using capillary pressure

D. Han

*Nanoelectronics Laboratory, Department of Electrical and Computer Engineering,
University of Cincinnati, Cincinnati, Ohio 45221-0030*

H. Li and T.M. Lu

*Department of Physics, Applied Physics, and Astronomy, Rensselaer Polytechnic Institute,
Troy, New York 12180-3590*

A.J. Steckl^{a)}

*Nanoelectronics Laboratory, Department of Electrical and Computer Engineering,
University of Cincinnati, Cincinnati, Ohio 45221-0030*

(Received 13 April 2010; accepted 9 June 2010)

Highly aligned microstrip patterns consisting of biaxial CaF₂ nanorods have been successfully self-assembled by simply using capillary pressure. The alignment direction of the microstrips is perpendicular to the flux direction during nanorod growth. Aligning behavior and pattern width can be controlled by changing wetting time and surface tension of the liquid. Higher surface tension and longer wetting time result in wider pattern width and better alignment. Taller nanorod height also results in better pattern alignment. Simple and cost-effective self-aligned microstrip patterns can be potentially used as a template for various applications, such as superhydrophobic surfaces, tissue scaffolds, microchannels, and optical polarizers.

I. INTRODUCTION

CaF₂ films with vertically aligned nanorods have been recently observed by Li et al.¹ These CaF₂ nanorods have been grown by using the oblique angle deposition technique.² The deposited nanorods present a unique microstructure due to shadowing and surface diffusion effects during the deposition process. Arrays of these CaF₂ nanorods, which possess a biaxial crystal orientation, can be grown on amorphous substrates, such as glass. Therefore, CaF₂ nanorod arrays can be potentially useful as buffer layers for production of high-quality semiconductor films.^{3,4} Similarly to other nanorods, such as carbon nanotubes⁵⁻⁷ and Si nanorods,⁸⁻¹¹ CaF₂ nanorods are also very susceptible to capillary pressure caused by liquid contact. We have investigated the effect of capillary pressure on the CaF₂ nanorods and, surprisingly, found that the CaF₂ nanorods array can be transformed into a uniaxially aligned microstrip structure by capillary pressure.

The effect of capillary pressure on vertically aligned nanorods has been intensively studied because it causes significant deformation of nanorod arrays due to their extremely high aspect ratio and surface-to-volume ratio. When a liquid droplet is placed on the nanorod array, nanorods are easily bundled or damaged. The bundling effect caused by liquid contact is normally an important

issue in various applications, especially for sensors and superhydrophobic surfaces. Therefore, this effect, also known as the “nanocarpet effect,”⁹ has been intensively studied to understand its underlying mechanism so that one can either eliminate or use the bundling of nanorod arrays.¹¹⁻¹³ Recently, some groups have reported periodic structures, such as cellular structure^{14,15} and hierarchical helical structures,¹⁶ resulting from capillary pressure. In this report, we demonstrate for the first time uniaxially self-aligned micropatterns induced by capillary pressure using CaF₂ nanorod arrays.

II. EXPERIMENTAL SECTION

A. Growth conditions of CaF₂ nanorods

The CaF₂ nanorods are grown by the oblique angle deposition technique in a vacuum chamber with a base pressure of 10⁻⁷ Torr. Glass slides or Si wafers are placed ~25 cm away from the CaF₂ source during deposition. The CaF₂ flux incident angle on the substrates was ~65° with respect to substrate normal. A quartz-microbalance device was used to monitor the growth rate and film thickness. Detailed growth conditions for CaF₂ nanorods can also be found elsewhere.¹

The as-deposited nanorods are nearly perpendicular to the substrate surface. The diameter of the nanorods is ~100 nm. The nanorod tip is sharp, with the slanted top surface nearly perpendicular to the incidence flux. Its four sidewalls are nearly parallel to the substrate normal. Overall, the film contains higher density (less porous)

^{a)}Address all correspondence to this author.

e-mail: a.steckl@uc.edu
DOI: 10.1557/jmr.2010.24

of nanorods perpendicular to the flux incident direction than that along the flux. On the basis of previous x-ray diffraction (XRD) analysis,¹ the films are known to be biaxially textured, denoted by $\{111\} \langle 121 \rangle$. Transmission electron microscopy (TEM) observations¹ performed in tandem with the XRD analysis revealed that taller nanorods have stronger biaxial orientation. The structure of individual nanorods and the overall morphology of a 1- μm -thick film are seen in Fig. 1. The biaxial structure at the tips of the nanorods is illustrated in Fig. 1(a). The nanorod density in the film is also dependent on the deposition flux direction. As seen in Fig. 1(b), there appears to be a greater number of channels free of nanorods in the direction perpendicular to the flux than in the direction parallel to the flux. The dark areas between high-density regions in Fig. 1(b) are caused by gaps between the tops of “tall” nanorods. As seen in Fig. 1(a), near the Si substrate these dark regions are populated with “short” nanorods that do not extend to the top because of shadowing effects during growth.

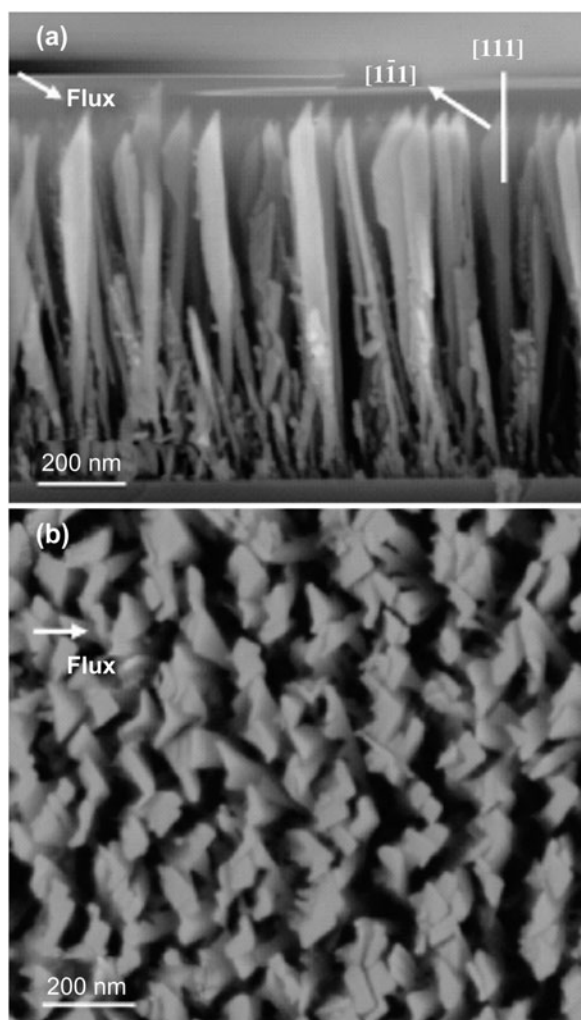


FIG. 1. SEM images of CaF₂ biaxial nanorods: (a) side view; (b) top view.

B. Contact angle measurement and SEM observation

A computer-interfaced VCA Optima XE goniometer (Advanced Surface Technology, Billerica, MA) was used for contact angle measurement. To measure water contact angles (WCA), a 2- μL water droplet was carefully placed onto the nanorod film. Because the water droplet spreads in an oval shape, WCAs are measured for both the short and long droplet dimensions. For scanning electron microscopy (SEM) observation, to minimize sample charging during electron microscopy all samples were coated with gold for 1 min at a pressure of 50 mTorr using a Desk II mini sputter machine (Denton Vacuum, Moorestown, NJ). SEM images were obtained using an SX-40A SEM system (ISI, Paramus, NJ).

C. Poly(dimethylsiloxane) (PDMS) casting

To replicate the aligned CaF₂ micropatterns, PDMS, Sylgard 184 (Dow Corning, Midland, MI), has been used for the casting process.¹⁷ Because of its viscoelastic liquid-like behavior, PDMS has to be mixed with its catalyst for solidification. After mixing PDMS and its catalyst at 10:1 volume ratio for 15 min, the mixed PDMS sol is placed into a vacuum oven for ~30 min to remove air bubbles. Before casting PDMS sol onto the master that has the aligned CaF₂ micropatterns, an antisticking monolayer is deposited onto the master surface by evaporating trimethylchlorosilane (TMCS) (Acros Organics, Geel, Belgium) for 10 min at room temperature. Next, PDMS sol is cast onto the master coated with the hydrophobic monolayer. After baking at 85 °C for 2 h in a conventional oven, PDMS sol is cured and solidified. Finally, the PDMS replica is peeled off from the master along the parallel direction to the aligned micropatterns.

III. RESULTS AND DISCUSSION

A water droplet placed on the biaxial CaF₂ nanorod array film spreads quickly and forms a directional (oval) shape. A watermark is observed after evaporation of the water droplet. This watermark exhibits diffracted light scattering similar to that observed with compact disks, indicating that a periodic micro/nanostructure has been formed. Figure 2 shows photos of the watermark and WCAs on a CaF₂ nanorod film. As shown in Figs. 2(a) and 2(b), the water droplet spreads directionally and the watermark remains in oval shape. The shadowing effect of oblique angle deposition results in higher nanorod density in the direction perpendicular to the flux than in the direction parallel to the flux, as seen in Fig. 1(b). Although the nanorods are not aligned at the microscopic level, the density difference provides a certain degree of aligned texture effect at the macroscopic level and results in anisotropic wetting caused by energy barrier difference to

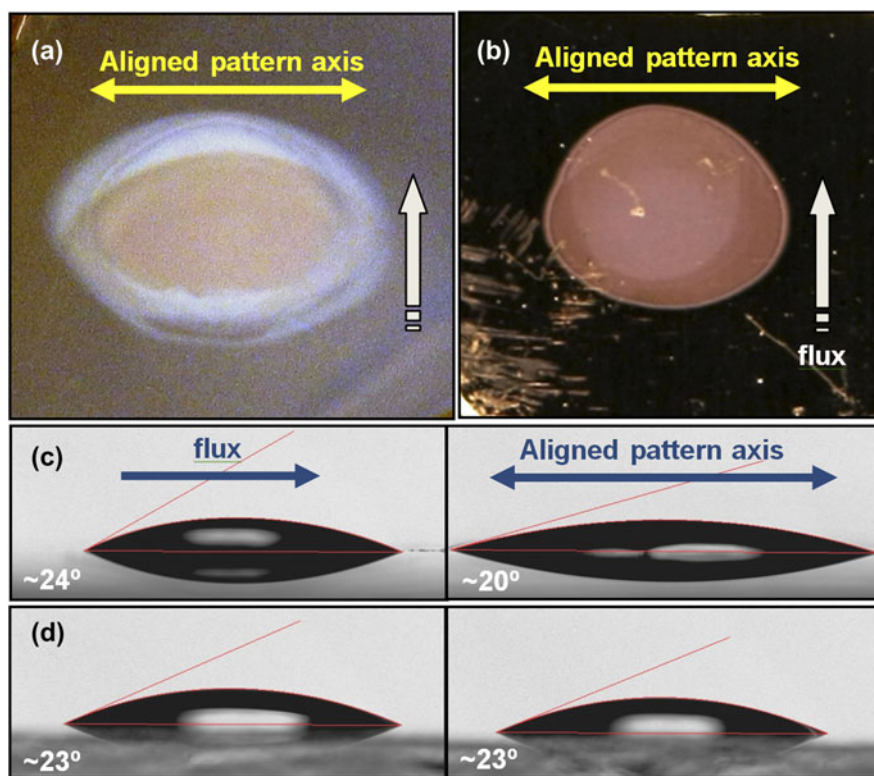


FIG. 2. Effect of water droplet: water mark photos on CaF₂ nanorod layers of (a) 1 μm and (b) 200 nm thickness; and WCA on (c) 1-μm-thick CaF₂ nanorod layer and on (d) CaF₂ film with no nanorods.

the movement of the water contact line.^{18,19} The directional spreading is proportionally related to the height of CaF₂ nanorods. Taller nanorods produce more directional spreading of the water droplet. The film of 1-μm-tall CaF₂ nanorods gives a very obvious oval shape of a watermark [Fig. 2(a)], whereas the film of 200-nm-tall CaF₂ nanorods gives an almost circular watermark [Fig. 2(b)]. The ratio between long and short axes in the two films is ~1.45:1 and 1.16:1, respectively. We have found that the long axis of the watermark is perpendicular to the flux incident direction for CaF₂ deposition. Because of this asymmetry distribution of water droplets, WCAs depend on the location of the measurement. For the film with nanorods of 1 μm in height [Fig. 2(c)], the WCA is ~24° on the location parallel to the flux direction and ~20° on the location perpendicular to the flux direction. In contrast, the WCA for the normally deposited CaF₂ film without the nanorods [Fig. 2(d)] is ~23° in all directions due to its circular spreading. From the watermark shape and its color based on the diffraction grating effect, we conclude that periodically aligned micro/nanopatterns must be formed after water treatment.

To confirm the formation of periodically aligned patterns after water treatment, we have investigated the watermark using electron microscopy. The original surface of the CaF₂ film with nanorod array has a relatively uniform morphology, as shown in Fig. 3(a). However, after the effect of capillary pressure exerted by a water

droplet the original uniform surface has been transformed into a patterned surface that consists of well-aligned microstrips [Fig. 3(b)] consisting of bundles of CaF₂ nanorods. Interestingly, the left edge of the strips [Fig. 3(c)] presents a different shape than the right edge. The SEM image of the cross section [Fig. 3(d)] reveals that the left edges are inclined while the right edges are nearly vertical. This difference has been observed in all microstrip patterns regardless of the direction of water intrusion and evaporation. It appears that the unique structure of CaF₂ nanorods results in the difference of edge morphology and pattern alignment.

On the rough surfaces of the nanorod array films, liquids are spread by capillary pressure²⁰ described by

$$P_c = \frac{2\gamma}{r_e} \cos \theta \quad , \quad (1)$$

where γ is the surface tension of the liquid, r_e is the effective radius of the interface, and θ is the contact angle between the solid and the liquid. Because the capillary pressure is closely related to the surface tension as described in Eq. (1), we have also investigated the effect of ethanol on the CaF₂ films with nanorod arrays. Ethanol has a much lower surface tension (22 mN/m) than water (72 mN/m). After ethanol evaporation, a pattern with aligned microstrips has also been observed, but their

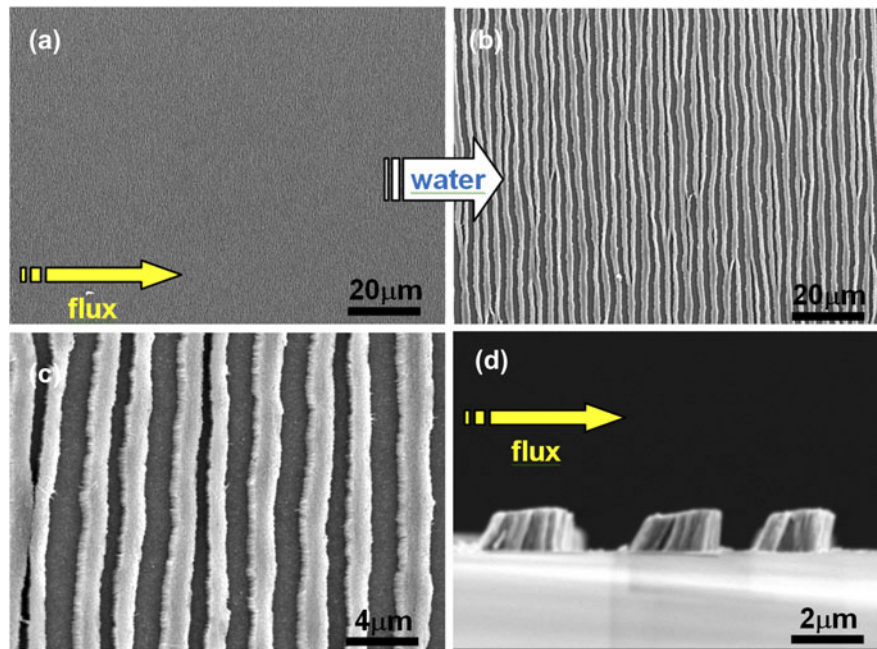


FIG. 3. SEM observation: (a) original surface of 1 μm tall CaF₂ nanorods (1 k× magnification); self-aligned microstrip patterns formed by water at (b) 1 k× and (c) 5 k× magnification; (d) cross-section view of microstrip patterns at 10 k×.

widths and alignment [Fig. 4(a)] are very different from that produced by water [Fig. 3(c)]. When the ethanol droplet is placed on the CaF₂ films with nanorod array, it wets a much larger area with a WCA ~0° because of its low surface tension and the high surface roughness. The microstrip width is thinner than that caused by water and the patterns are not aligned very well. Similarly, for shorter nanorods of 200 nm, much less well-aligned microstrips are formed [Fig. 4(b)].

Optical microscope observation has been performed to investigate the transition of CaF₂ nanorod array into aligned microstrips. As shown schematically in Figs. 5(a) and 5(b), three different regions have been identified after placing a water droplet onto the film with nanorod arrays. Regions A and B are wetted by the initial water droplet and the capillary-driven water intrusion, respectively. Region C is the dried area where aligned microstrips are formed. Figures 5(c)–5(e) show the real-time transition of CaF₂ nanorod film into an aligned microstrip pattern. When the water droplet is placed onto the CaF₂ films with nanorod arrays, the area wetted by the water droplet is constant for an initial period of time and then becomes smaller as the water evaporates. The area wetted by capillary pressure also becomes smaller as its boundary area is drying and transitions to self-assembled microstrips. Interestingly, no transition has been observed in any region while it is wet, whereas it suddenly occurs when the wet surface is drying out. A video clip taken at 200× of the microstrip formation process is included as Supplementary Information. In this

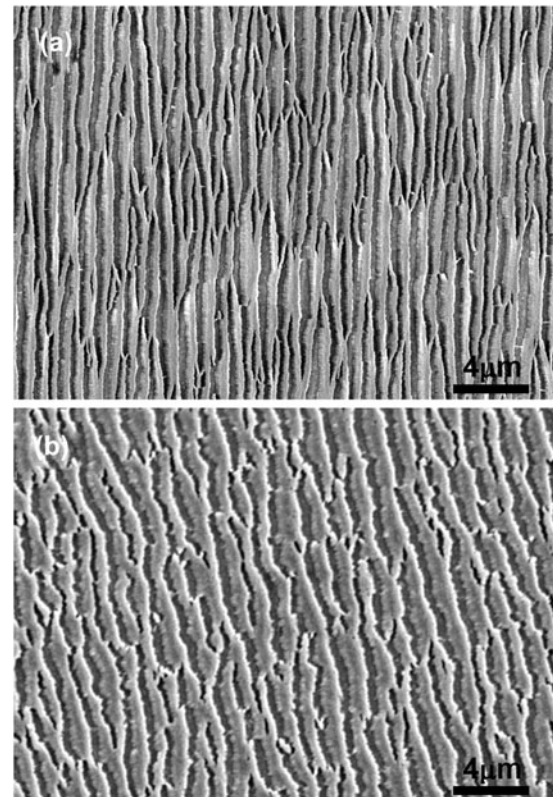


FIG. 4. SEM observation of (a) self-aligned microstrip patterns formed by ethanol; (b) self-aligned microstrip patterns of 200 nm tall CaF₂ nanorods formed by water.

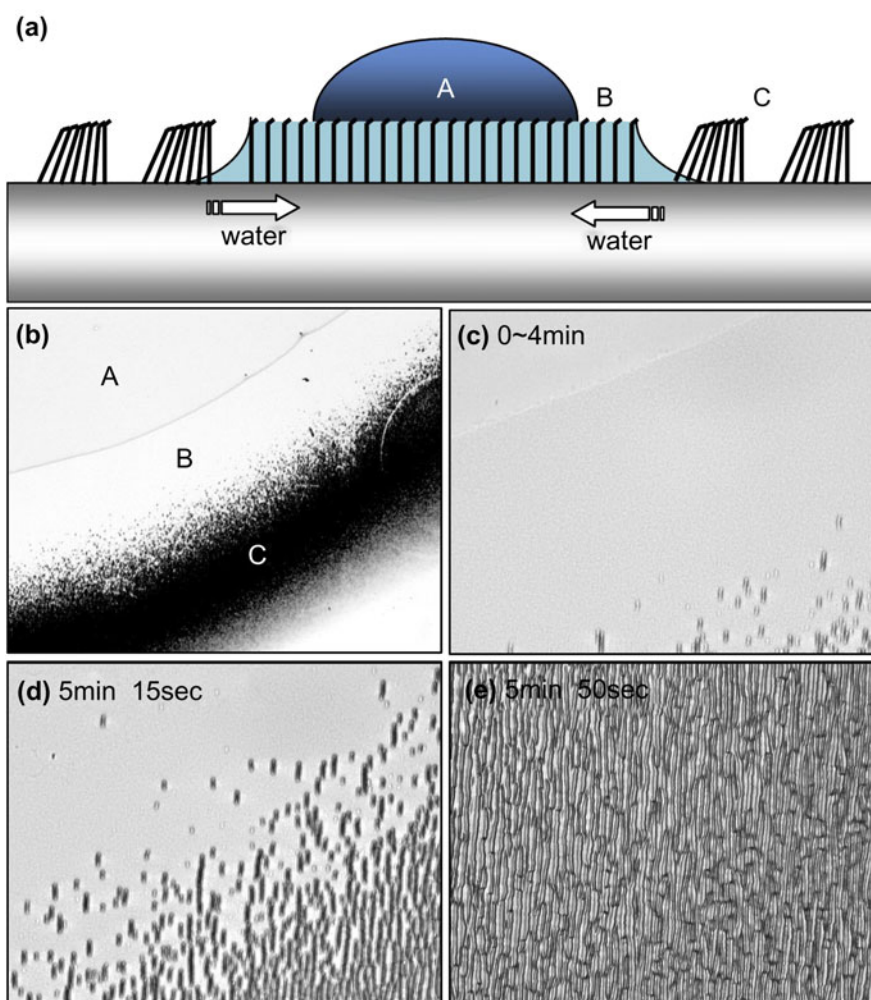


FIG. 5. Optical microscope observation: (a) schematic diagram for self-aligned pattern formation. (b) A and B regions wet by water droplet and capillary-driven water, respectively, and the dried C region has self-aligned microstrip patterns ($100\times$ magnification); (c) maintaining initial status from water droplet displacement ($400\times$ magnification); (d) self-assembling microstrip patterns in drying area ($400\times$ magnification); (e) dry surface that has microstrip patterns ($400\times$ magnification).

video, initially a portion of the water droplet is seen retreating in the left side at some distance from the microstrips. Microstrip formation follows the retreating water droplet, but only in the region where the below-surface water is evaporating.

The difference in the micropattern resulting from the use of ethanol [Fig. 4(a)] may be due not only to the low surface tension of ethanol but also because the ethanol droplet evaporates very quickly due to its higher vapor pressure and larger wetted surface area. Even for the water droplet case, the width of the microstrips in the center region of the watermark is wider than that in the boundary area, which may be caused by differences in wetting time. To control the effect of wetting time, instead of using evaporating liquid droplets the CaF₂ nanorod films have been dipped into the solution for certain times ranging from 10 s to 10 min and then dried with weak nitrogen blow. Both water and ethanol were used to examine the surface tension effect.

The resulting width of the microstrips is plotted in Fig. 6 as a function of wetting time. For ethanol wetting, the microstrip width did not change significantly with wetting time. On the other hand, for water the width increased considerably with wetting time. The difference in microstrip width between water and ethanol is not significant at a short wetting time (1 min). However, it becomes obvious at longer time periods. Higher surface tension and longer wetting time provide wider microstrip widths and better alignment. As demonstrated, the ability to control aligning behavior and microstrip width can be accomplished by changing wetting time and by selecting liquids with different surface tension. Simple and cost-effective self-aligned micro/nanopatterns can potentially be used as templates for superhydrophobic surfaces, tissue scaffolds, microchannels, optical polarizers, etc.

Using this simple and cost-effective self-aligned microstructure as a template, PDMS replicas have been

successfully produced by PDMS casting as shown in Fig. 7(a). Because PDMS is a hydrophobic material that has low surface tension ~ 20 mN/m and high WCA $\sim 118^\circ$ [right side droplet in Fig. 7(b)], patterned PDMS replicas provide improved hydrophobicity induced by the surface roughness. As shown in Fig. 7(b), two different WCAs

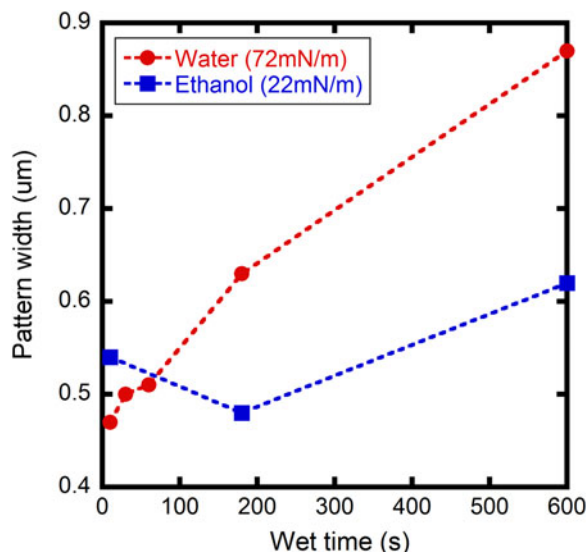


FIG. 6. Capillary pressure effect: microstrip width versus wetting time of water/ethanol.

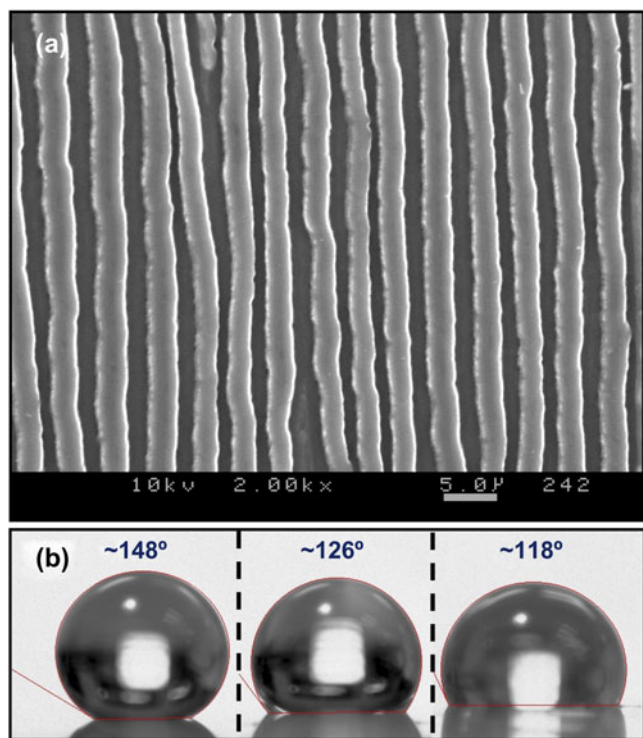


FIG. 7. PDMS cast on CaF₂ film: (a) SEM of patterned CaF₂ film and PDMS template. (b) Contact angles on different axis of negative PDMS duplicate: parallel view to alignment axis (left), perpendicular view to alignment axis (middle), and on smooth PDMS film (right).

have been measured on locations either parallel or perpendicular to the axis of pattern alignment. WCA of the left side droplet $\sim 148^\circ$ in Fig. 7(b) has been measured from the viewpoint of the parallel axis [i.e., upper/lower side on Fig. 5(a)], whereas the WCA of the center droplet of $\sim 126^\circ$ has been measured from the viewpoint of the perpendicular axis [i.e., left/right side on Fig. 5(a)]. By simple geometric calculation based on the approximated value of 2- μ m microstrip width, 1- μ m gap width, and 1- μ m nanorod height, its roughness factor on the parallel axis is ~ 1.7 . Using the Wenzel equation, the calculated contact angle is $\sim 143^\circ$, which is close to the measured contact angle $\sim 148^\circ$. Because the surface roughness can be increased by using a thinner pattern width and the taller nanorods, a superhydrophobic surface with aligned texture can be accomplished.

The formation of the microstrips may be related to the interaction of the capillary force with the biaxial structure and placement of the nanorods. However, identifying the specific process by which nanorods are selectively moved to form microstrips perpendicular to the deposition flux direction has been difficult to pinpoint. Interestingly, the geometric relationship between the microstrips and the flux direction is found at all positions of the periphery of the droplet. Therefore, the withdrawal direction of the water as it evaporates does not play a determining role. Finally, the microstrips themselves exhibit an asymmetry in cross section, with only nanorods at the “windward” side of the microstrip are tilted away from the deposition flux. This must be related to the biaxial structure of the nanorods, as the nanorod tip contains a tilted {111} surface.

IV. CONCLUSION

Using capillary pressure of liquids, uniaxially self-aligned microstrip patterns of CaF₂ films with nanorod arrays have been demonstrated. This is a simple and cost-effective method to produce aligned micropatterns. Further research will focus on producing improved alignment for use in microfluidic applications and the fabrication of superhydrophobic surfaces by controlling pattern dimensions. The underlying transition mechanism of nanorod-induced microstrips will also be investigated further.

ACKNOWLEDGMENTS

The work is supported in part at Rensselaer by National Science Foundation (NSF) Grant No. 0506738 and at Cincinnati by a Dayton Area Graduate Studies Institute (DAGSI) grant.

REFERENCES

- H.F. Li, T. Parker, F. Tang, G.C. Wang, T.M. Lu, and S. Lee: Biaxially oriented CaF₂ films on amorphous substrates. *J. Cryst. Growth* **310**, 3610 (2008).

2. Y. Zhao, D. Ye, G-C. Wang, and T-M. Lu: Designing nanostructures by glancing angle deposition, in *Proceedings of the 48th SPIE Annual Meeting*, Vol. 5219 (SPIE, San Diego, CA, 2003), p. 59.
3. A.T. Findikoglu, W. Choi, V. Matias, T.G. Holesinger, Q.X. Jia, and D.E. Peterson: Well-oriented silicon thin films with high carrier mobility on polycrystalline substrates. *Adv. Mater.* **17**, 1527 (2005).
4. C.W. Teplin, D.S. Ginley, and H.M. Branz: A new approach to thin film crystal silicon on glass: Biaxially-textured silicon on foreign template layers. *J. Non-Cryst. Solids* **352**, 984 (2006).
5. H. Liu, S. Li, J. Zhai, H. Li, Q. Zheng, L. Jiang, and D. Zhu: Self-assembly of large-scale micropatterns on aligned carbon nanotube films. *Angew. Chem. Int. Ed.* **43**, 1146 (2004).
6. K.K.S. Lau, J. Bico, K.B.K. Teo, M. Chhowalla, G.A.J. Amaratunga, W.I. Milne, G.H. McKinley, and K.K. Gleason: Superhydrophobic carbon nanotube forests. *Nano Lett.* **3**, 1701 (2003).
7. C. Journet, S. Moulinet, C. Ybert, S.T. Purcell, and L. Bocquet: Contact-angle measurements on superhydrophobic carbon nanotube forests: Effect of fluid pressure. *Europhys. Lett.* **71**, 104 (2005).
8. J.G. Fan and Y.P. Zhao: Characterization of watermarks formed in nano-carpet effect. *Langmuir* **22**, 3662 (2006).
9. J.G. Fan, D. Dyer, G. Zhang, and Y.P. Zhao: Nanocarpet effect: Pattern formation during the wetting of vertically aligned nanorod arrays. *Nano Lett.* **4**, 2133 (2004).
10. J.G. Fan and Y.P. Zhao: Spreading of a water droplet on a vertically aligned Si nanorod array surface. *Appl. Phys. Lett.* **90**, 013102 (2007).
11. J.G. Fan and Y.P. Zhao: Freezing a water droplet on an aligned Si nanorod array substrate. *Nanotechnology* **19**, 155707 (2008).
12. D. Chandra and S. Yang: Capillary-force-induced clustering of micropillar arrays: Is it caused by isolated capillary bridges or by the lateral capillary meniscus interaction force? *Langmuir* **25**, 10430 (2009).
13. J.G. Fan, J.X. Fu, A. Collins, and Y.P. Zhao: The effect of the shape of nanorod arrays on the nanocarpet effect. *Nanotechnology* **19**, 045713 (2008).
14. N. Chakrapani, B. Wei, A. Carrillo, P.M. Ajayan, and R.S. Kane: Capillarity-driven assembly of two-dimensional cellular carbon nanotube foams. *Proc. Natl. Acad. Sci. USA* **101**, 4009 (2004).
15. X. Huang, J.J. Zhou, E. Sansom, M. Gharib, and S.C. Haur: Inherent-opening-controlled pattern formation in carbon nanotube arrays. *Nanotechnology* **18**, 305301 (2007).
16. B. Pokroy, S.H. Kang, L. Mahadevan, and J. Aizenberg: Self-organization of a mesoscale bristle into ordered, hierarchical helical assemblies. *Science* **323**, 237 (2009).
17. M. Sun, C. Luo, L. Xu, H. Ji, Q. Ouyang, D. Yu, and Y. Chen: Artificial lotus leaf by nanocasting. *Langmuir* **21**, 8978 (2005).
18. J.Y. Chung, J.P. Youngblood, and C.M. Stafford: Anisotropic wetting on tunable micro-wrinkled surfaces. *Soft Matter* **3**, 1163 (2007).
19. K. Khare, J. Zhou, and S. Yang: Tunable open-channel microfluidics on soft poly(dimethylsiloxane) (PDMS) substrates with sinusoidal grooves. *Langmuir* **25**, 12794 (2009).
20. E.W. Washburn: The dynamics of capillary flow. *Phys. Rev.* **17**, 273 (1921).